Frontiers in Bioscience Landmark

Front. Biosci. (Landmark Ed) **2026**; 31(2): 47168
https://doi.org/10.31083/FBL47168

Original Research

Insulin-Like Growth Factor 1 in Exosomes Derived from Adipose-Derived Stem Cells Promotes Tendon-Bone Healing in Rotator Cuff Injuries

Wenxiao Qi[1,†], Yiren Jin[1,†], Haojie Shan[1], Ye Lu[1], Feng Wang[1,*]

[1]Department of Orthopaedic Surgery, Shanghai Jiao Tong University Affiliated Sixth People's Hospital, 200233 Shanghai, China
*Correspondence: wf_online@163.com (Feng Wang)
[†]These authors contributed equally.

Academic Editor: Elisa Belluzzi
Submitted: 8 October 2025 Revised: 4 January 2026 Accepted: 16 January 2026 Published: 6 February 2026

Abstract

Background: Rotator cuff injuries are common musculoskeletal disorders and are frequently complicated by impaired tendon–bone healing and high re-tear rates after surgical repair. Exosomes derived from adipose-derived stem cells (ADSCs) have shown regenerative potential through paracrine mechanisms; however, the role of exosomal insulin-like growth factor 1 (IGF1) in tendon–bone healing remains unclear. **Methods**: Exosomes were isolated from rat ADSCs with or without lentiviral knockdown of IGF1. A rat supraspinatus tendon tear and repair model was established, and 200 μg of exosomes was administered systemically post-surgery. Tendon–bone healing was evaluated at 8 weeks post-operation using histological, immunohistochemical, and micro-computed tomography analyses. Early molecular responses were assessed at 1-week post-surgery by Western blot and RT-qPCR. Angiogenic markers (vascular endothelial growth factor (VEGF), CD31, α-SMA), inflammatory cytokines (interleukin (IL)-1β, IL-18), pyroptosis-related proteins (gasdermin D N-terminal fragment (GSDMD-N)), and NLRP3 inflammasome components were examined. **Results**: ADSC-derived exosomes significantly enhanced bone mineral density, fibrocartilage formation, vascularization, and biomechanical strength at the tendon–bone interface. These effects were accompanied by reduced inflammatory cytokine expression, inhibition of pyroptosis, and suppression of NLRP3 inflammasome activation. In contrast, exosomes derived from IGF1-deficient ADSCs exhibited markedly reduced therapeutic efficacy, with attenuated angiogenic, anti-inflammatory, and anti-pyroptotic effects. **Conclusions**: Exosomal IGF1 plays a critical role in promoting angiogenesis, suppressing inflammation and pyroptosis, and improving structural and biomechanical outcomes during tendon–bone healing. IGF1-enriched ADSC-derived exosomes represent a promising therapeutic strategy for enhancing rotator cuff repair.

Keywords: rotator cuff injuries; exosomes; adipose-derived stem cells; insulin-like growth factor 1; tendon-bone healing

1. Introduction

The rotator cuff is a complex anatomical structure composed of four tendons that stabilize the glenohumeral joint and facilitate normal shoulder motion [1]. Rotator cuff injuries are among the most common musculoskeletal disorders, particularly in individuals engaged in repetitive overhead activities and in aging populations [2]. These injuries range from tendinopathy and partial-thickness tears to full-thickness tendon ruptures, leading to pain, weakness, restricted range of motion, and functional impairment [3]. Despite advancements in surgical and non-surgical treatment modalities, rotator cuff tears present a significant clinical challenge due to persistently high rates of re-tear and suboptimal tendon-to-bone healing [4]. Consequently, current research is increasingly focused on understanding the biological environment of the tendon, enhancing regenerative approaches, and developing novel biomaterials to improve clinical outcomes [5].

Adipose-derived stem cells (ADSCs) have emerged as a promising source of mesenchymal stem cells (MSCs) with significant potential in regenerative medicine and tissue engineering [6]. Isolated from the stromal vascular fraction of adipose tissue, ADSCs exhibit multilineage differentiation capacity, immunomodulatory properties, and a high proliferative profile [7]. Compared with other MSC sources, such as bone marrow, ADSCs offer advantages including minimal invasiveness during harvest, higher yield, and reduced donor site morbidity [8]. ADSCs exert therapeutic effects not only through their differentiation capacity but also, increasingly, via paracrine mechanisms-especially by releasing extracellular vesicles (EVs), such as exosomes [9]. Exosomes are nanoscale vesicles (30–150 nm in diameter) derived from the endosomal pathway, which serve as carriers of bioactive components, including proteins, lipids, mRNAs, and microRNAs [10]. These vesicles mediate intercellular communication and play a critical role in regulating inflammation, stimulating angiogenesis, preventing apoptosis, and supporting tissue regeneration [11].

ADSC-derived exosomes (ADSC-exo) are gaining attention as a cell-free therapeutic modality that recapitulates many of the regenerative effects of stem cell trans-

plantation without the associated risks of tumorigenicity, immune rejection, or vascular occlusion [12,13]. Accordingly, in this study, our objective is to investigate the effects of ADSC-exo on angiogenesis, inflammation, and pyroptosis at the tendon-bone interface during rotator cuff repair, and to evaluate their potential to enhance rotator cuff healing after surgical repair. Furthermore, we aim to elucidate the role of the key protein insulin-like growth factor 1 (IGF1) contained within ADSC-exo.

2. Methods

2.1 Isolation and Culture of Rat ADSCs

ADSCs were isolated from the inguinal adipose tissue of 4-week-old Sprague-Dawley rats according to the protocol described in previous research [14], and the rats were euthanized in the same manner as in Section 2.6. Briefly, adipose tissue was harvested under sterile conditions, minced into approximately 1-mm^3 fragments, and enzymatically digested with collagenase. The digested suspension was filtered, centrifuged, and the resulting cell pellet was resuspended and cultured in complete culture medium. Cells were maintained at 37 °C in a humidified atmosphere containing 5% CO_2, and medium was refreshed every 2–3 days. ADSCs at passage 3 were used for all subsequent experiments. All primary ADSCs were validated for cell identity by surface marker analysis using flow cytometry and were confirmed to be mycoplasma-negative, ensuring the reliability and reproducibility of the experimental results.

2.2 Lentiviral-Mediated Knockdown of Igf1 in ADSCs

To suppress IGF1 expression, ADSCs were transduced with lentiviral vectors encoding short hairpin RNA (shRNA) targeting rat Igf1 (GenePharma, Shanghai, China). The shRNA sequence targeting Igf1 was GGTGGATGCTCTTCAGTTC, while a non-targeting sequence (ACTTACGCTGAGTACTTCG) served as the negative control. Lentiviral transduction was performed according to the manufacturer's instructions. Knockdown efficiency was confirmed at both mRNA and protein levels.

2.3 Exosome Isolation and Characterization

Exosomes were isolated from ADSC-conditioned medium using a standard differential ultracentrifugation protocol. Briefly, culture supernatants were sequentially centrifuged at 1000 ×g for 10 min to remove cells and debris, 10,000 ×g for 30 min to eliminate large extracellular vesicles, and 100,000 ×g for 70 min to pellet exosomes. The resulting pellet was resuspended in phosphate-buffered saline (PBS) and further purified by filtration through a 0.22-µm membrane. Exosome morphology was examined by transmission electron microscopy (TEM), and particle size distribution and concentration were determined using nanoparticle tracking analysis (NTA). Expression of canonical exosomal markers (Tsg101, CD63, and CD9) was assessed by Western blotting. Exosomal protein concentration was measured using a bicinchoninic acid (BCA) protein assay according to the manufacturer's instructions.

Exosome purity was evaluated by calculating the particle-to-protein ratio (particles/µg protein).

2.4 Assessment of ADSC Viability After IGF1 Knockdown

To evaluate whether IGF1 knockdown affects ADSC viability, a Cell Counting Kit-8 (CCK-8) assay was performed. Control ADSCs and IGF1-knockdown ADSCs (shIGF1) in the logarithmic growth phase were seeded into 96-well plates at a density of 5×10^3 cell/well in 100 µL complete culture medium containing 10% fetal bovine serum. Cell viability was assessed on days 1, 2, 3, and 4 after seeding by adding CCK-8 reagent according to the manufacturer's instructions. Absorbance was measured at 450 nm using a microplate reader, and relative cell viability was calculated for each time point.

2.5 In Vivo Biodistribution of Systemically Administered Exosomes

To evaluate whether systemically administered exosomes can reach the tendon–bone injury site, exosome biodistribution was assessed using DiI fluorescent labeling. Purified ADSC-derived exosomes were incubated with the lipophilic fluorescent dye DiI at a final concentration of 5 µM for 30 min at 4 °C in the dark. To remove unbound dye, the labeled exosomes were ultracentrifuged at 100,000 ×g for 70 min and resuspended in sterile PBS.

DiI-labeled exosomes were administered to rats with rotator cuff tear via tail-vein injection. Three days after injection, rats were euthanized in the same manner as in Section 2.6, and tendon tissues from the repair site were harvested, embedded, sectioned, and examined under a fluorescence microscope to detect DiI fluorescence signals.

2.6 Rat Rotator Cuff Tear Model and Exosome Administration

The rat rotator cuff tear and repair model were established following the surgical procedure described in previous research [15,16]. A total of 42 adult female Sprague–Dawley rats (4–5 months old, 258–552 g) were used. Animals were randomly assigned to experimental groups using a computer-generated random number table. Investigators performing outcome assessments were blinded to group allocation. General anesthesia was induced with 2–3% isoflurane in 100% oxygen. A transverse incision was made lateral to the deltoid muscle to expose the rotator cuff complex. The supraspinatus tendon was sharply detached from the greater tuberosity, and the footprint was gently debrided to simulate clinical tendon avulsion prior to repair.

Postoperatively, 200 µg of ADSC-derived exosomes suspended in 200 µL PBS were administered via tail vein injection immediately after surgery (day 0), on days 3 and 7, and once weekly thereafter until the designated endpoints.

Animals were euthanized at 1 or 8 weeks post-surgery under deep anesthesia by intraperitoneal injection of sodium pentobarbital (150 mg/kg). Death was confirmed by the absence of respiration, corneal reflex, and heartbeat.

2.7 Western Blot

At 1 week post-surgery, tendon tissues from the repair site were harvested and homogenized in RIPA lysis buffer. Protein samples were separated by SDS–PAGE and transferred to PVDF membranes. Membranes were incubated with primary antibodies against IGF1 (1:2000, #ab322659, Abcam, Cambridge, MA, USA), VEGFA (1:1000, #ab214424, Abcam), CD31 (1:1500, #ab222783, Abcam), interleukin (IL)-1β (1:1000, Ag10295, Proteintech, Wuhan, China), IL-18 (1:1000, 30587-1-AP, Proteintech), ACTA2 (1:1500, #19245, Cell Signaling Technology, Danvers, MA, USA), and GAPDH (#1:2000, 60004-1-Ig, Proteintech) (used as an internal control), followed by HRP-conjugated secondary antibodies. Protein bands were visualized using enhanced chemiluminescence.

2.8 Quantitative Real-Time PCR (qRT-PCR)

qRT-PCR was performed using SYBR Green Master Mix (#4344463, Thermo Fisher Scientific, Waltham, MA, USA) on a CFX96 Real-Time PCR System (Bio-Rad, Hercules, CA, USA). *GAPDH* was used as the internal reference gene. The primer sequences used were as follows:

GAPDH:
F: 5′-TCAAGAAGGTGGTGAAGCAG-3′;
R: 5′-GGTGGAAGAGTGGGAGTTGC-3′.
Igf1:
F: 5′-CCTGCTTGCTCACCTTTACC-3′;
R: 5′-GGTAGCTCAGGCATGTCCAG-3′.
Vegfa:
F: 5′-GAGAGGTACAGTGCTGCCCT-3′;
R: 5′-CACACAGGACGGCTTGAAGA-3′.
Acta2:
F: 5′-GACCTTGAGAAGAGTTACGAGTTG-3′;
R: 5′-TAGAGAGACAGCACGATGGG-3′.
Cd31:
F: 5′-GCTGGTGCTGTTCTTCCTGT-3′;
R: 5′-AGGTGCCATCCAGGTACTTG-3′.
Il18:
F: 5′-TGCCATGTCAGAAGACTCTGC-3′;
R: 5′-TGGGTCACAGCCAGTTCTTC-3′.
Il1b:
F: 5′-TGCAGCTGGAGAGTGTGGAT-3′;
R: 5′-TGTCGTTGCTTGGTTCTCCT-3′.

2.9 Histological and Immunohistochemical Analysis

At 8 weeks post-surgery, shoulder joint specimens were fixed in 4% paraformaldehyde, decalcified, embedded in paraffin, and sectioned at 5-µm thickness. Hematoxylin and eosin (H&E) staining was used to assess overall tissue morphology, while Safranin O–Fast Green staining was performed to evaluate fibrocartilage formation at the tendon–bone interface. For immunohistochemistry, sections were incubated with primary antibodies against VEGF, followed by secondary antibodies and DAB visualization to assess neovascularization.

2.10 Micro-CT and Biomechanical Testing

Micro-computed tomography (micro-CT) analysis was conducted to assess bone structure and mineralization at the greater tuberosity [17]. Following scanning, 3D reconstruction was used to evaluate bone volume parameters and trabecular architecture. For biomechanical testing, the humerus-tendon-scapula complex was harvested and subjected to uniaxial tensile loading to determine maximum load to failure and stiffness, thereby assessing the mechanical integrity of the tendon-to-bone repair.

2.11 Statistical Analysis

All data are presented as mean $\pm$ standard deviation (SD). Normality was assessed using the Shapiro–Wilk test. As data were normally distributed but exhibited unequal variances among groups, Brown–Forsythe ANOVA and Welch's correction were applied where appropriate. For pairwise comparisons, Welch's *t*-test was used. Actual F values, t values, effect sizes, and sample sizes (n) are reported in the Results section and corresponding figure legends. Statistical analyses were performed using GraphPad Prism version 9.0 (GraphPad Software, San Diego, CA, USA), and $p < 0.05$ was considered statistically significant.

3. Results

3.1 Inhibition of Igf1 in ADSCs Reduces IGF1 Expression in Derived Exosomes

To verify whether IGF1 knockdown affected ADSC viability, a CCK-8 assay was performed to assess cell viability. From day 1 to day 4 of culture, the relative cell viability of control ADSCs and shIGF1-transduced ADSCs increased in parallel, and no significant differences were observed at any time point (day 4: t = 0.87, df = 10, p = 0.483, Cohen's d = 0.30; **Supplementary Fig. 1**). These results demonstrate that IGF1 knockdown did not impair ADSC viability.

To determine whether suppression of Igf1 in ADSCs altered IGF1 expression and its incorporation into secreted exosomes, ADSCs were transduced with lentiviral shRNA targeting *Igf1*. Quantitative RT-PCR and Western blot analyses confirmed a significant reduction in *Igf1* mRNA and IGF1 protein levels in shIGF1-transduced ADSCs compared with controls (Fig. 1A–C; $p < 0.01$, Brown–Forsythe ANOVA; F = 14.25, df = 2.6, partial $\eta^2 = 0.83$ for Fig. 1A; F = 11.89, df = 2.6, partial $\eta^2 = 0.80$ for Fig. 1C).

Exosomes isolated from control and shIGF1 ADSCs were subsequently characterized. Western blotting further confirmed the presence of canonical exosomal markers TSG101, CD63, and CD9, with no detectable differences

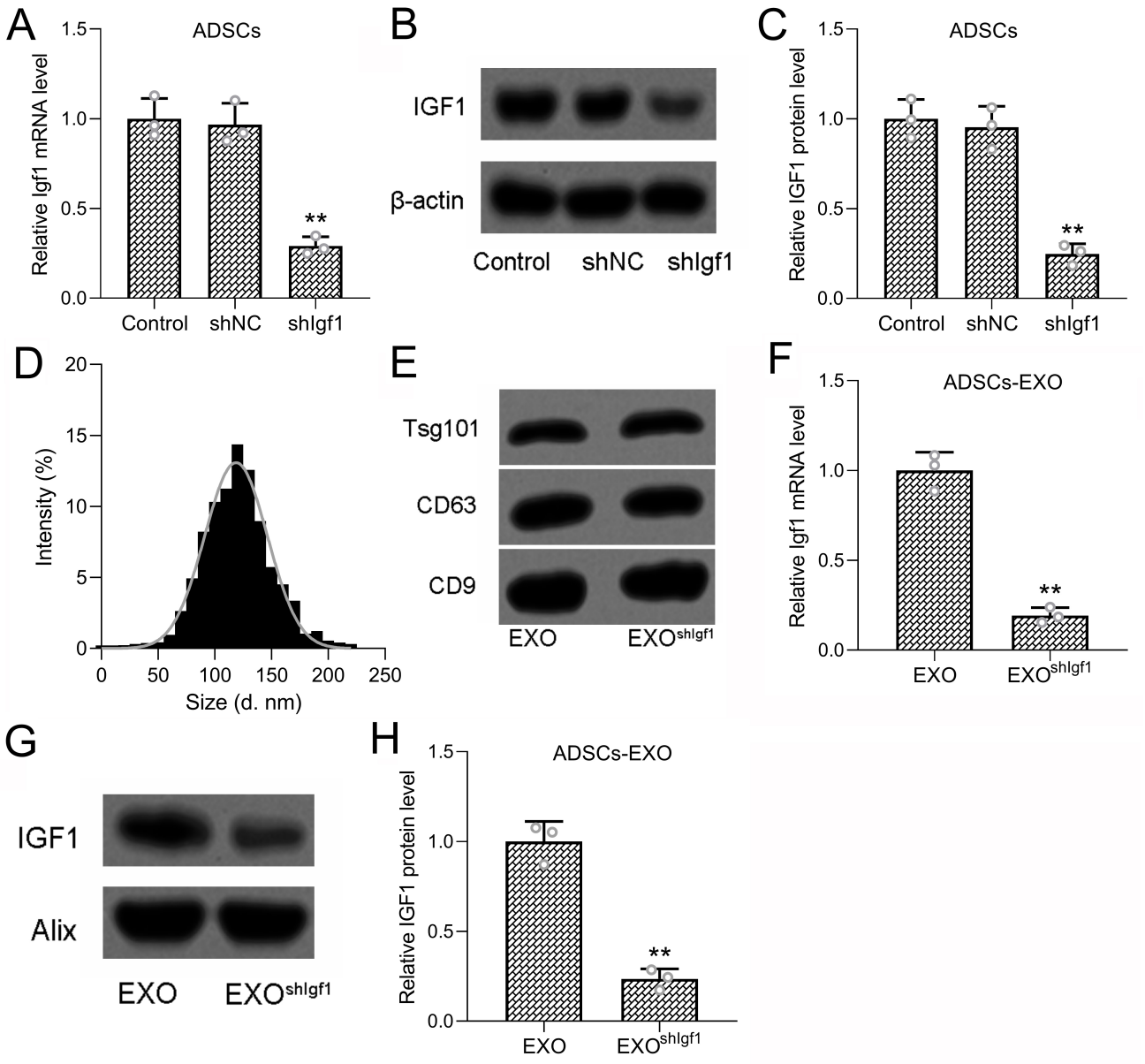

Fig. 1. Inhibition of Igf1 in ADSCs attenuated the content of IGF1 in ADSCs derived exosomes. (A) ADSCs were transfected with shIgf1 for 48 hours, the mRNA and protein expressions of IGF1 were measured (B,C). 3 repeats were conducted. (D) Size distribution of the exosomes derived from ADSCs with Igf1 inhibition. (E) Detection of Tsg101, CD63, CD9 expressions by Western blotting analysis from exosomes derived from ADSCs and ADSCs with Igf1 inhibition. (F) Detection of *Igf1* mRNA expressions by qRT-PCR from exosomes derived from ADSCs and ADSCs with Igf1 inhibition. (G,H) Detection of IGF1 and Alix protein expressions by Western blotting analysis from exosomes derived from ADSCs and ADSCs with Igf1 inhibition. 3 repeats were conducted. Data was shown with mean ± SD. $^{**}p < 0.01$ compared to control (or EXO group as control). Brown–Forsythe ANOVA test and Unpaired *t* test with Welch's correction. IGF1, insulin-like growth factor 1; ADSCs, adipose-derived stem cells; Tsg101, tumor susceptibility gene 101; qRT-PCR, Quantitative Real-Time PCR; SD, standard deviation; EXO, exosomes; ANOVA, analysis of variance.

between control and shIGF1-derived exosomes (Fig. 1D,E), indicating that Igf1 knockdown did not affect exosome biogenesis or structural integrity. To further evaluate whether Igf1 knockdown affects exosome yield and purity, particle concentration and total protein content of isolated exosomes were quantified, and the particle-to-protein ratio was calculated. No significant differences were observed between control ADSC-derived exosomes (EXO) and Igf1-knockdown ADSC-derived exosomes (EXO^{shIGF1}) in particle concentration, protein concentration, or particle-to-protein ratio (**Supplementary Fig. 2A–C**). These results further indicate that Igf1 knockdown does not affect basic exosome biogenesis, yield, or purity, but specifically reduces IGF1 cargo within the exosomes.

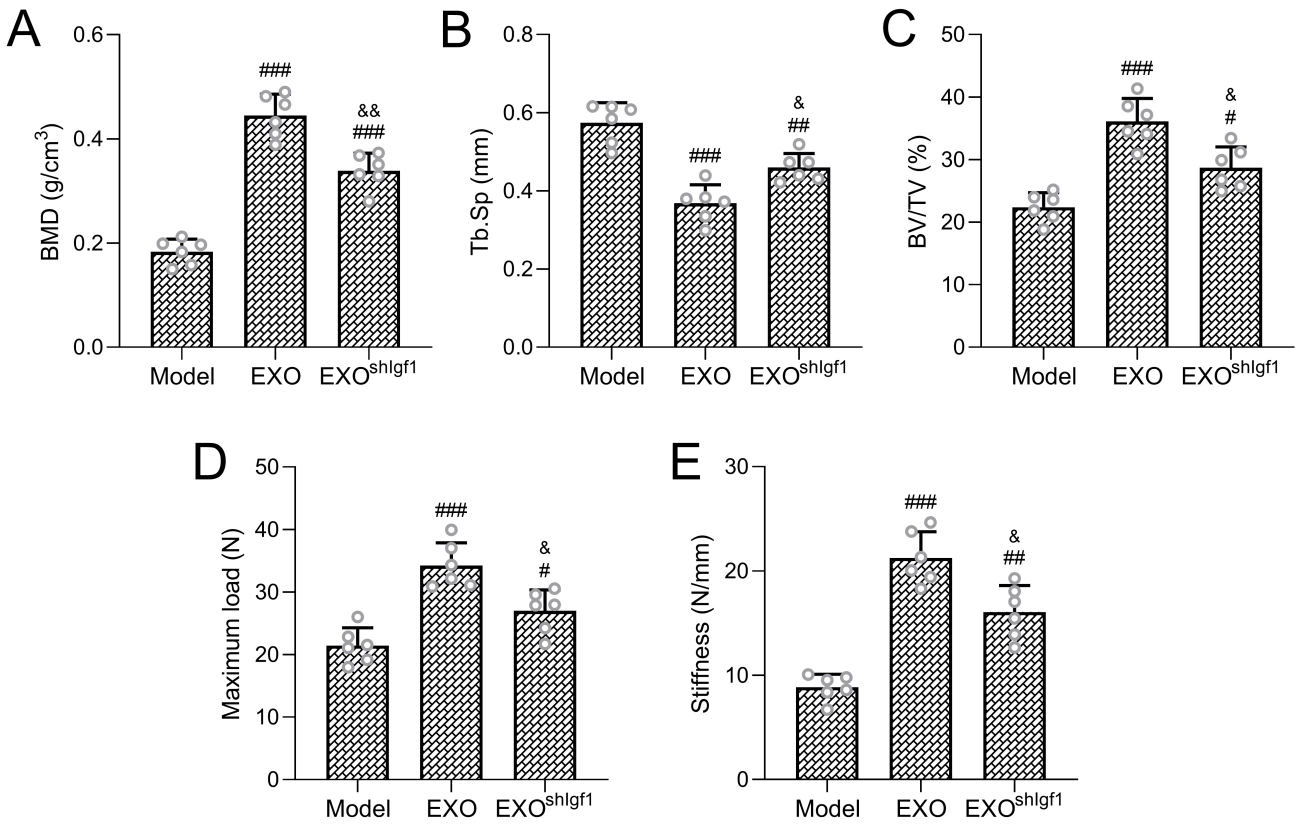

Fig. 2. Therapeutic efficacy in rotator cuff repair. Micro-computed tomography was used to evaluate bone remodeling at the tendon–bone interface, including bone mineral density (BMD; A), trabecular separation (Tb.Sp; B), and bone volume fraction (BV/TV; C). Mechanical properties of the repaired rotator cuff were assessed by measuring ultimate failure load (D) and stiffness (E). Six rats were included in each experimental group. Data are shown as mean ± SD. Statistical analysis was performed using Brown–Forsythe ANOVA followed by Dunnett's T3 post hoc test. #$p < 0.05$, ##$p < 0.01$, ###$p < 0.001$ versus the Model group; &$p < 0.05$, &&$p < 0.01$ versus the EXO group.

Importantly, analysis of exosomal cargo revealed a substantial reduction in IGF1 content following Igf1 knockdown. qRT-PCR demonstrated significantly decreased *Igf1* mRNA levels in exosomes derived from shIGF1-transduced ADSCs compared with controls (Fig. 1F; $p < 0.01$, independent-samples *t*-test; t = 4.68, df = 4, Cohen's d = 1.91). Consistently, Western blot analysis showed a pronounced reduction in IGF1 protein levels in shIGF1-derived exosomes, while the exosomal protein Alix remained unchanged and served as a loading control (Fig. 1G,H; independent-samples *t*-test; t = 4.02, df = 4, Cohen's d = 1.65). Collectively, these results demonstrate that lentiviral-mediated Igf1 knockdown specifically reduces IGF1 expression in ADSCs and concomitantly decreases IGF1 mRNA and protein content in their secreted exosomes, without altering ADSC viability or fundamental exosome biogenesis. These findings establish a robust foundation for subsequent functional analyses of IGF1-deficient exosomes in tendon–bone healing.

3.2 Exosomes From Igf1-Deficient ADSCs Exhibit Reduced Therapeutic Efficacy in Rotator Cuff Repair

Given that exosomes were administered systemically in this study, it was first necessary to determine whether intravenously delivered exosomes could reach the tendon–bone injury site. Accordingly, DiI-labeled ADSC-derived exosomes were injected via the tail vein. Distinct DiI fluorescence signals were detected in tendon tissues three days after injection, indicating that systemically delivered exosomes are able to successfully reach and persist at the injury site (**Supplementary Fig. 3**).

To assess the structural and functional outcomes of rotator cuff repair, micro-CT and biomechanical analyses were performed at 8 weeks post-surgery. Micro-CT analysis demonstrated that treatment with exosomes derived from control ADSCs (EXO group) significantly improved bone microarchitecture at the tendon–bone interface compared with the untreated model group (**Supplementary Fig. 4**). Specifically, bone mineral density (BMD), bone volume fraction (BV/TV), and trabecular spacing (Tb.Sp) were all significantly improved in the EXO group (Fig. 2A–C;

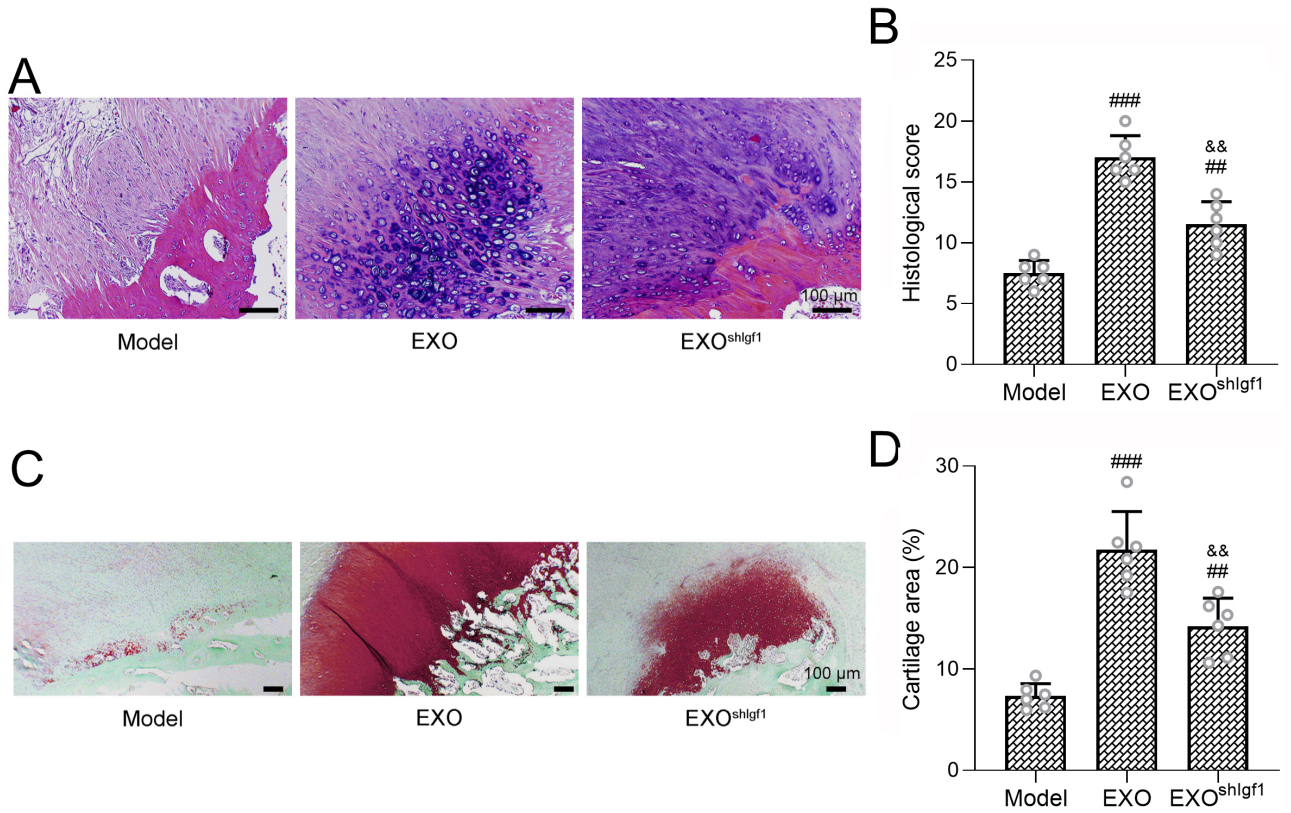

Fig. 3. Tissue organization and fibrocartilage formation at the repair site. (A) Representative histological sections stained with hematoxylin and eosin (H&E), and (B) quantitative evaluation of overall histological scores. Scale bar = 100 μm. (C) Representative Safranin O–Fast green (SO–FG), and (D) Safranin O–positive cartilage area. Scale bar = 100 μm. Six rats were included in each group. Results are expressed as mean ± SD. ##$p < 0.01$, ###$p < 0.001$ versus the Model group; &&$p < 0.01$ versus the EXO group. Statistical significance was determined using Brown–Forsythe ANOVA followed by Dunnett's T3 multiple comparisons test.

Brown–Forsythe ANOVA: F = 20.37, df = 2.15, partial η^2 = 0.73 for BMD; F = 16.52, df = 2.15, partial η^2 = 0.68 for BV/TV; F = 18.45, df = 2.15, partial η^2 = 0.71 for Tb.Sp). In contrast, these osteogenic benefits were markedly attenuated when exosomes were derived from Igf1-knockdown ADSCs. Compared with the EXO group, the shIGF1-EXO group exhibited significantly reduced BMD and BV/TV, along with increased Tb.Sp, indicating compromised bone regeneration at the tendon–bone interface.

Consistent with the micro-CT findings, biomechanical testing revealed that the maximum load to failure and interfacial stiffness were significantly higher in the EXO group than in the untreated model group, confirming enhanced mechanical integration of the repaired tendon (Fig. 2D,E; Brown–Forsythe ANOVA: F = 22.68, df = 2.15, partial η^2 = 0.75 for maximum load; F = 17.93, df = 2.15, partial η^2 = 0.70 for stiffness). However, both biomechanical parameters were significantly reduced in the shIGF1-EXO group relative to the EXO group. Taken together, these results indicate that IGF1 deficiency substantially compromises the ability of ADSC-derived exosomes to promote bone regeneration and mechanical restoration at the tendon–bone interface, supporting a critical role for exosomal IGF1 mediating the therapeutic efficacy of exosome-based treatment in rotator cuff repair.

3.3 Igf1 Knockdown in ADSC-Derived Exosomes Impairs Their Histological Benefits on Tendon–Bone Healing

To further evaluate histological remodeling at the tendon–bone interface following rotator cuff repair, H&E staining and SO–FG staining were performed on specimens harvested 8 weeks post-surgery. Significantly lower scores were revealed in the EXO group compared with the model group, indicating reduced inflammatory features and more orderly fibrocartilage structure (Fig. 3A,B; Brown–Forsythe ANOVA: F = 16.82, df = 2.15, partial η^2 = 0.69). Consistently, SO–FG staining demonstrated a significantly greater cartilage area in the EXO group relative to the model group (Fig. 3C,D; Brown–Forsythe ANOVA: F = 19.75, df = 2.15, partial η^2 = 0.72). In contrast, exosomes derived from Igf1-deficient ADSCs (shIGF1-EXO group) failed to reproduce these histological benefits. Both histological scores and Safranin O–positive cartilage areas were significantly reduced compared with the EXO group, indicating impaired fibrocartilage regeneration and suboptimal structural integration. Collectively, these findings demonstrate

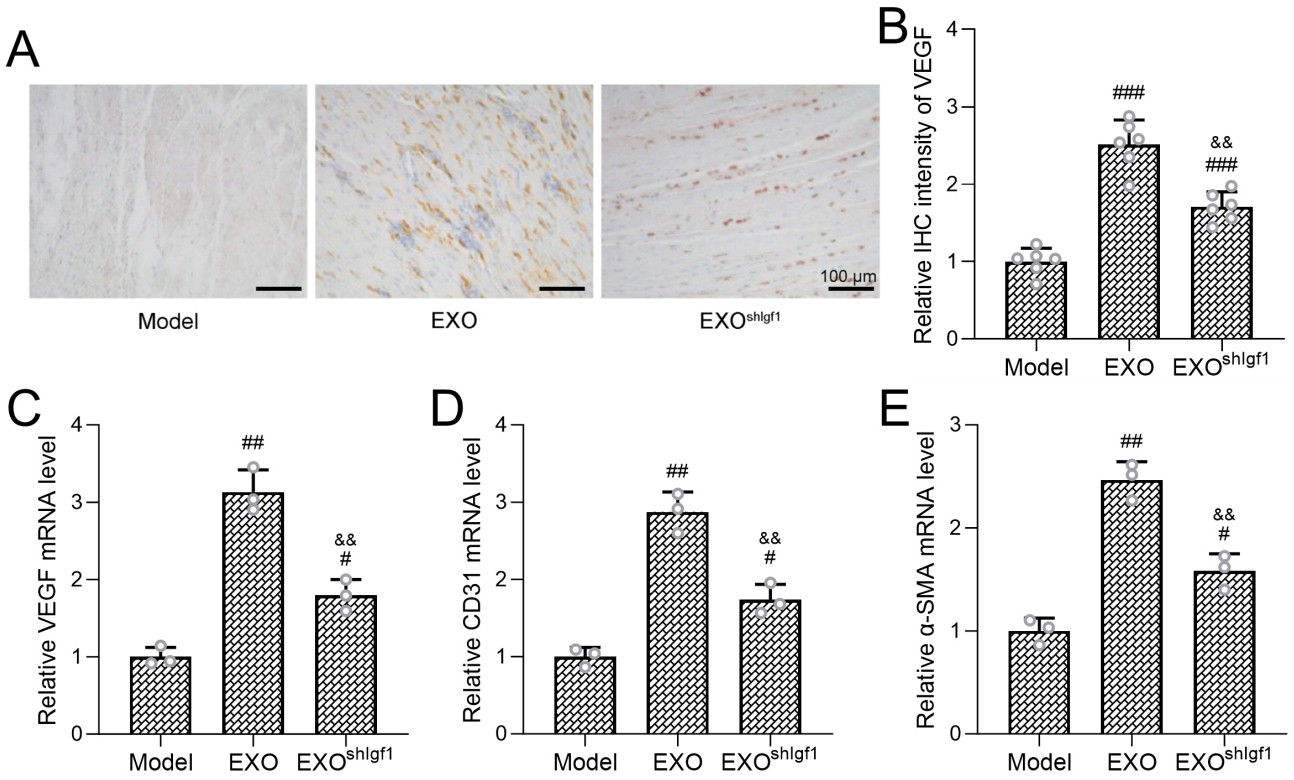

Fig. 4. Igf1 Deficiency decreases exosome' pro-angiogenic effects in rotator cuff repair. (A) Representative images of immunohistochemical staining of vascular endothelial growth factor (VEGF), and (B) intensity of VEGF in tendon tissues. Scale bar = 100 μm. Transcriptional levels of angiogenesis-related genes, including *Vegfa* (C), *Cd31* (D), and *α-SMA* (E), were assessed in tendon tissues by RT-qPCR. Six rats were included per group, and RT-qPCR analyses were performed using pooled tissue homogenates with three independent repeats. Data are expressed as mean ± SD. #$p < 0.05$, ##$p < 0.01$, ###$p < 0.001$ versus the Model group; &&$p < 0.01$ versus the EXO group. Statistical comparisons were conducted using Brown–Forsythe ANOVA followed by Dunnett's T3 post hoc test.

that IGF1 is a critical mediator of exosome-driven histological repair and chondrogenesis at the tendon–bone interface during rotator cuff healing.

3.4 Igf1 Deficiency in ADSC-Derived Exosomes Weakens Their Pro-Angiogenic Effects in Rotator Cuff Repair

To investigate the contribution of ADSC-derived exosomes to angiogenesis during tendon–bone healing, immunohistochemical staining and gene expression analyses were performed on tendon tissues harvested 8 weeks after surgery. A significant increase in VEGF-positive staining was demonstrated in the EXO group (Fig. 4A,B, Brown–Forsythe ANOVA, F = 14.92, df = 2.15, partial η^2 = 0.66). Consistent with the IHC findings, RT-qPCR analysis demonstrated that exosome treatment significantly upregulated the mRNA expression levels of *Vegfa* (Fig. 4C, Brown–Forsythe ANOVA, F = 12.38, df = 2.6, partial η^2 = 0.80), *Cd31* (Fig. 4D, Brown–Forsythe ANOVA, F = 11.75, df = 2.6, partial η^2 = 0.79), and *α-SMA* (Fig. 4E, Brown–Forsythe ANOVA, F = 10.52, df = 2.6, partial η^2 = 0.78) in tendon tissues, further supporting enhanced angiogenic activity.

In contrast, the pro-angiogenic responses were substantially attenuated when exosomes were derived from Igf1-deficient ADSCs. Compared with the EXO group, the shIGF1-EXO group exhibited significantly reduced VEGF staining intensity as well as lower transcript levels of *Vegfa*, *Cd31*, and *Acta2*. These findings indicate that IGF1 plays a critical role in mediating the angiogenic activity of ADSC-derived exosomes in the context of rotator cuff repair.

3.5 Igf1-Deficient Exosomes Exhibit Reduced Inhibitory Effects on Pyroptosis in Rotator Cuff Tendon Tissue

To evaluate the effects of ADSC-derived exosomes on tendon cell pyroptosis following rotator cuff injury, tendon tissues were harvested 1 week after surgery for propidium iodide (PI) staining and Western blot analysis. A sham-operated group was included as a baseline control. Compared with the sham group, the untreated model group exhibited a marked increase in PI-positive cells, indicating enhanced pyroptotic activity in the injured tendon tissue (Fig. 5A,B). Treatment with exosomes derived from control ADSCs (EXO group) significantly reduced the number of PI-positive cells relative to the model group, suggesting an inhibitory effect of exosomes on tendon cell pyroptosis

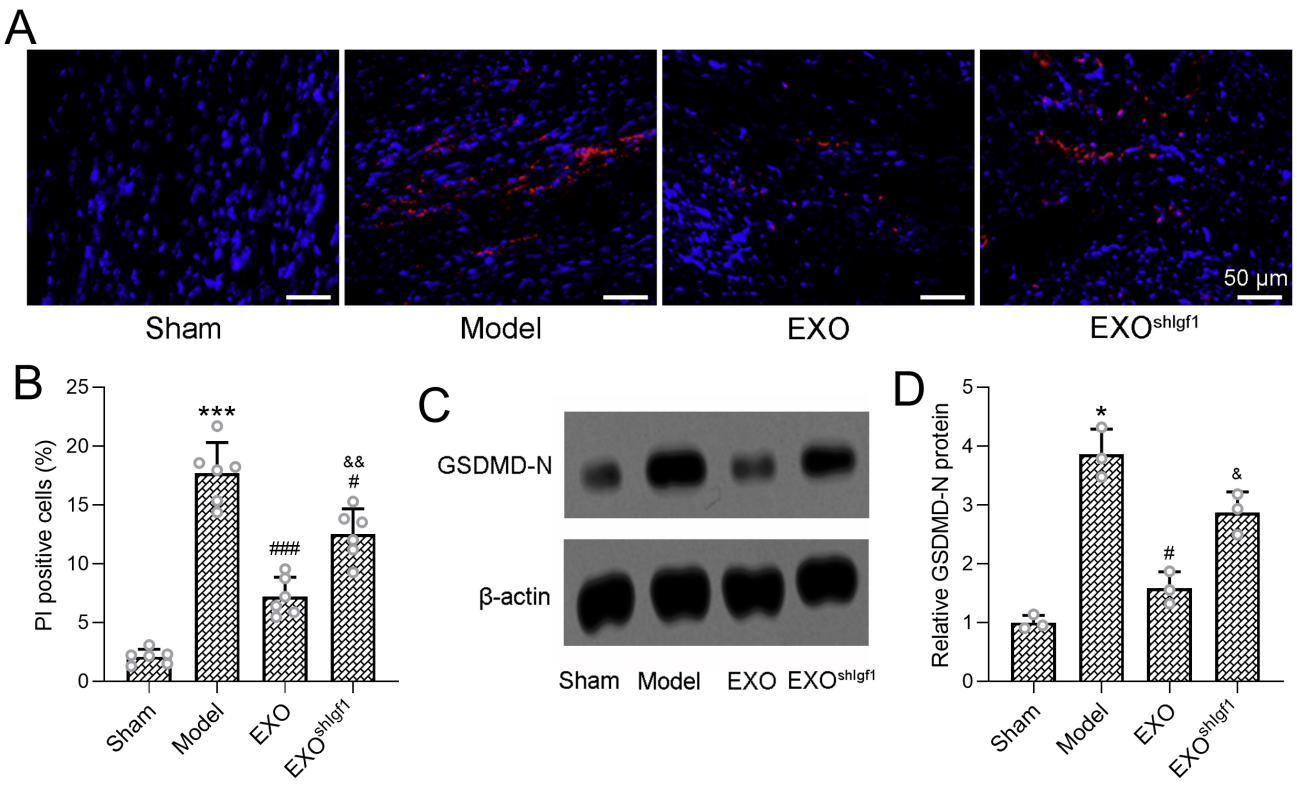

Fig. 5. Igf1-deficient exosomes exhibit reduced inhibitory effects on pyroptosis. (A) Representative propidium iodide (PI) fluorescence staining of tendon sections, and (B) quantitative analysis revealed PI-positive cells in membrane-compromised cells. Scale bar = 50 μm. Protein expression of the pyroptosis executor gasdermin D N-terminal fragment (GSDMD-N) in tendon tissues was assessed by Western blotting (C). β-actin served as an internal loading control, and protein levels were normalized to the sham group (D). Six rats were included per group, and Western blot analyses were performed using pooled tendon tissue homogenates with three independent repeats. Data are presented as mean ± SD. *$p < 0.05$, ***$p < 0.001$ versus the Sham group; #$p < 0.05$, ###$p < 0.001$ versus the Model group; &$p < 0.05$, &&$p < 0.01$ versus the EXO group. Statistical analysis was conducted using Brown–Forsythe ANOVA followed by Dunnett's T3 multiple comparisons test.

during the early healing phase (Fig. 5B; Brown–Forsythe ANOVA: F = 17.25, df = 3.20, partial $\eta^2 = 0.73$).

Consistent with these findings, Western blot analysis demonstrated a pronounced upregulation of gasdermin D N-terminal fragment (GSDMD-N), a key executor of pyroptosis, in the model group, whereas exosome treatment markedly suppressed GSDMD-N expression toward baseline levels (Fig. 5C). Quantitative analysis of GSDMD-N normalized to β-actin further confirmed this reduction (Fig. 5D; Brown–Forsythe ANOVA: F = 13.89, df = 3.8, partial $\eta^2 = 0.84$).

Notably, the anti-pyroptotic effects of exosome treatment were significantly attenuated when exosomes were derived from Igf1-knockdown ADSCs. Compared with the EXO group, the shIGF1-EXO group exhibited a higher proportion of PI-positive cells and significantly elevated GSDMD-N protein levels. These results indicate that IGF1 is required for the exosome-mediated suppression of tendon cell pyroptosis during the early stage of rotator cuff healing.

3.6 Igf1 Knockdown Attenuates the Anti-Inflammatory Effects of ADSC-Derived Exosomes in Rotator Cuff Injury

To further examine the regulatory effects of ADSC-derived exosomes on the inflammatory response associated with NLRP3 inflammasome activation and pyroptosis, the protein and mRNA expression levels of the pro-inflammatory cytokines IL-1β and IL-18 were assessed in tendon tissues one week after rotator cuff injury (Fig. 6A–D). Compared with the sham-operated group, the untreated model group exhibited significantly elevated protein levels of IL-1β and IL-18, reflecting a robust inflammatory response during the early healing phase (Fig. 6A,B; Brown–Forsythe ANOVA: F = 14.23, df = 3.20, partial $\eta^2 = 0.71$ for IL-1β; F = 12.85, df = 3.20, partial $\eta^2 = 0.68$ for IL-18). Treatment with exosomes derived from control ADSCs (EXO group) significantly reduced the protein levels of both IL-1β and IL-18 compared with the model group, indicating a pronounced anti-inflammatory effect of exosome therapy. Consistent with the protein expression data, RT-qPCR analysis demonstrated similar trends at the transcriptional level. The mRNA expression of Il1b and Il18

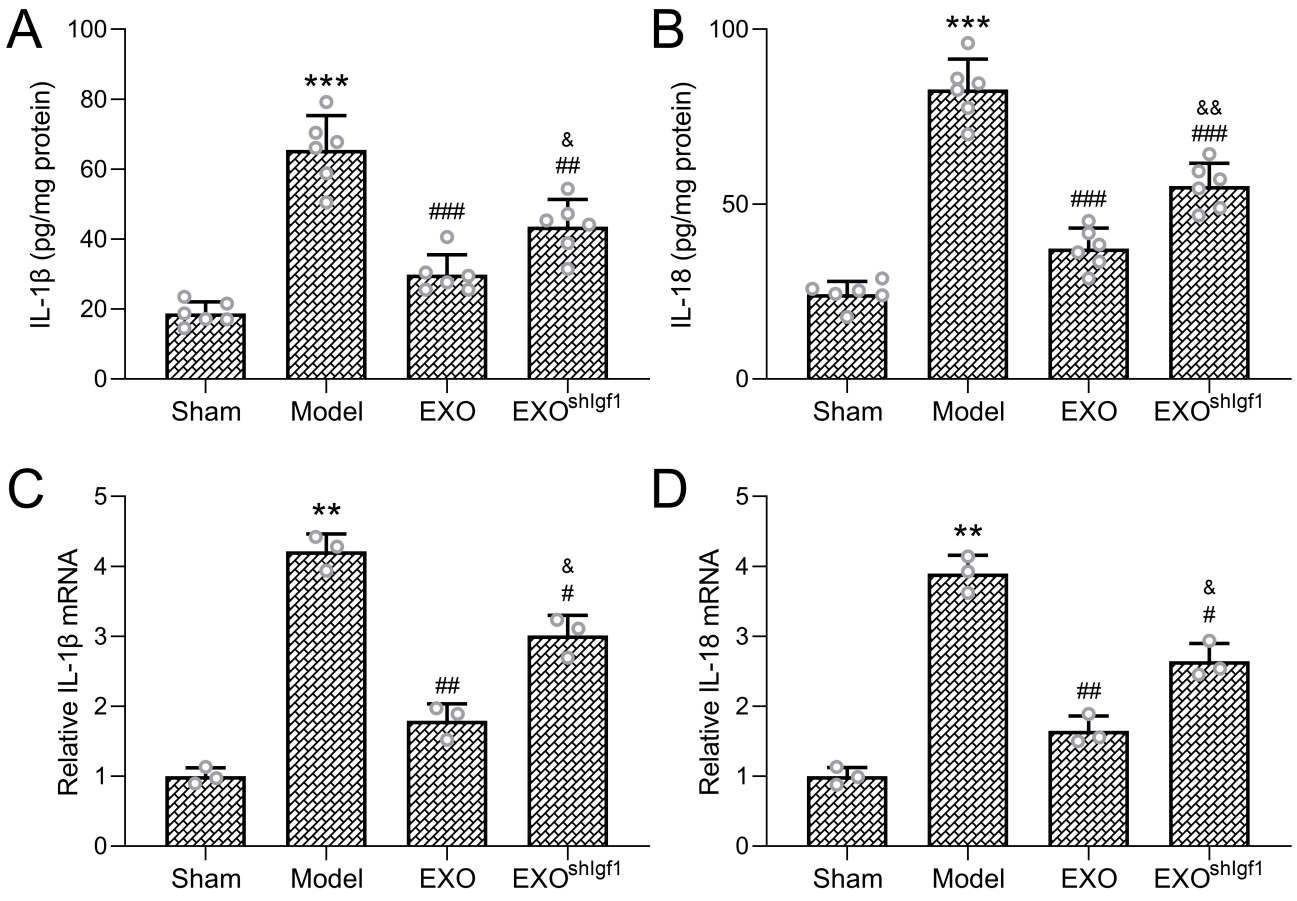

Fig. 6. Igf1 Knockdown attenuates the anti-inflammatory effects. Protein concentrations of the pro-inflammatory cytokines interleukin-1β (IL-1β; A) and interleukin-18 (IL-18; B) in tendon tissues were quantified by enzyme-linked immunosorbent assay (ELISA). Transcriptional expression of *Il1b* (C) and *Il18* (D) was determined by RT-qPCR. Six rats were included per group, and RT-qPCR analyses were performed using pooled tendon tissue homogenates with three independent repeats. Results are presented as mean $\pm$ SD. $^{**}p < 0.01$, $^{***}p < 0.001$ versus the Sham group; $\#p < 0.05$, $\#\#p < 0.01$, $\#\#\#p < 0.001$ versus the Model group; $\&p < 0.05$, $\&\&p < 0.01$ versus the EXO group. Statistical significance was assessed using Brown–Forsythe ANOVA followed by Dunnett's T3 multiple comparisons test.

was markedly upregulated in the model group but significantly suppressed following exosome treatment (Fig. 6C,D; Brown–Forsythe ANOVA: F = 10.87, df = 3.8, partial η^2 = 0.79 for *Il1b*; F = 9.52, df = 3.8, partial η^2 = 0.77 for *Il18*).

Notably, these anti-inflammatory effects were substantially attenuated when exosomes were derived from Igf1-inhibited ADSCs. Compared with the EXO group, the shIGF1-EXO group exhibited significantly higher levels of IL-1β and IL-18 at both the protein and mRNA levels. These findings indicate that IGF1 plays a key role in mediating the immunomodulatory properties of ADSC-derived exosomes during the early inflammatory phase of rotator cuff tendon healing.

3.7 Igf1 Deficiency Impairs the Inhibitory Effect of ADSC-Derived Exosomes on NLRP3 Inflammasome Activation

To investigate the influence of ADSC-derived exosomes on NLRP3 inflammasome activation in the early phase of tendon healing, Western blot analysis was performed on tendon tissues collected one-week post-surgery. The NLRP3 inflammasome is a critical innate immune signaling complex that detects pathogenic stimuli or cellular stress. Once activated, NLRP3 recruits the adaptor protein ASC through PYD–PYD interactions. ASC then facilitates the conversion of pro-caspase-1 into its active form, triggering the release of pro-inflammatory cytokines and initiating pyroptosis [18–20]. Compared to the sham group, the model group showed marked upregulation of NLRP3 (Fig. 7A,B, Brown–Forsythe ANOVA, F = 13.25, df = 3.8, partial η^2 = 0.83), ASC (Fig. 7A,C, Brown–Forsythe ANOVA, F = 12.18, df = 3.8, partial η^2 = 0.81), pro-caspase-1 (Fig. 7A,D, Brown–Forsythe ANOVA, F = 10.92, df = 3.8, partial η^2 = 0.79), and cleaved caspase-1 protein levels (Fig. 7A,E, Brown–Forsythe ANOVA, F = 14.57, df = 3.8, partial η^2 = 0.85), indicating robust inflammasome activation ($p < 0.01$).

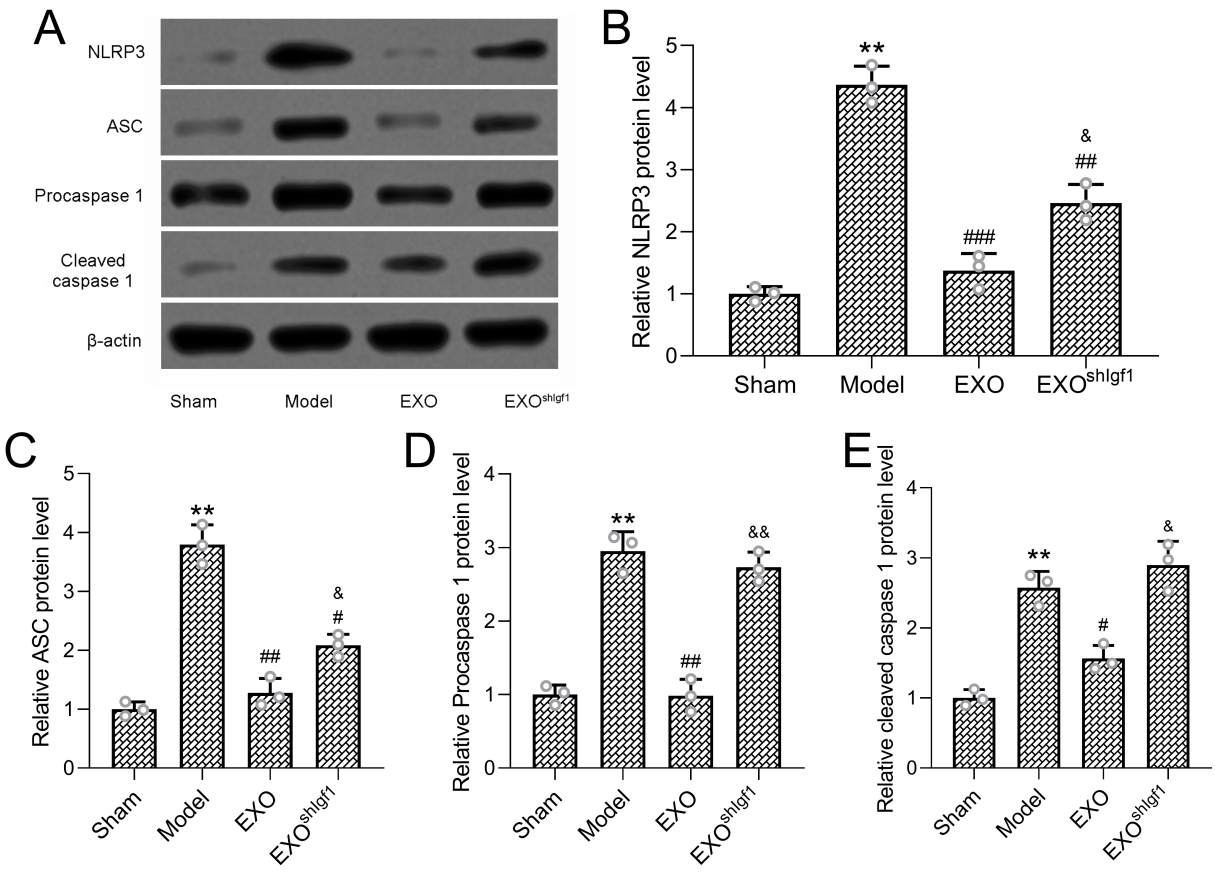

Fig. 7. Effect of ADSC-Derived exosomes on NLRP3 inflammasome activation. Protein levels of NLRP3 inflammasome–related components, including NLRP3, ASC, pro-caspase-1, and cleaved caspase-1, were examined in tendon tissues by Western blot analysis (A). β-actin served as the internal loading control, and band intensities were quantified and normalized to the sham group (B–E). Six rats were included in each experimental group, and Western blot analyses were performed using pooled tendon tissue homogenates with three independent replicates. Data are expressed as mean $\pm$ SD. $^{**}p < 0.01$ versus the Sham group; $\#p < 0.05$, $\#\#p < 0.01$, $\#\#\#p < 0.001$ versus the Model group; $\&p < 0.05$, $\&\&p < 0.01$ versus the EXO group. Statistical comparisons were conducted using Brown–Forsythe ANOVA followed by Dunnett's T3 post hoc test. NLRP3, NOD-like receptor pyrin domain-containing protein 3; ASC, Apoptosis-associated speck-like protein containing a C-terminal caspase recruitment domain.

Treatment with exosomes derived from control ADSCs (EXO group) significantly suppressed the expression of these inflammasome-related proteins compared with the model group, indicating effective inhibition of NLRP3 inflammasome activation. In contrast, this suppressive effect was markedly attenuated when exosomes were derived from Igf1-knockdown ADSCs. Compared with the EXO group, the shIGF1-EXO group exhibited significantly higher levels of NLRP3, ASC, and cleaved caspase-1, demonstrating incomplete inhibition of inflammasome signaling.

Collectively, these findings indicate that IGF1 is essential for the ability of ADSC-derived exosomes to suppress NLRP3 inflammasome activation during the early inflammatory phase of rotator cuff tendon healing, thereby linking exosomal IGF1 to coordinated regulation of inflammation, pyroptosis, and tissue repair.

4. Discussion

In the present study, we demonstrate that exosomes derived from rat ADSCs significantly promote tendon–bone healing in a rat model of rotator cuff injury. Importantly, our findings indicate that these therapeutic effects are mediated, at least in part, by IGF1 contained within the exosomes. ADSC-derived exosomes promoted structural regeneration, and angiogenesis, while concurrently suppressing inflammation and pyroptosis. Notably, exosomes derived from IGF1-silenced ADSCs exhibited markedly reduced therapeutic efficacy, supporting a critical functional role for IGF1 in exosome-mediated tendon–bone repair.

Rotator cuff injuries often result in incomplete healing due to insufficient biological reattachment between tendon and bone, leading to high rates of re-tear [21]. Conventional surgical repair methods restore anatomical continuity but do not adequately address the biological deficien-

cies at the repair interface [22]. Our results support the use of ADSC-derived exosomes as a promising cell-free regenerative strategy capable of enhancing the biological healing response. Exosome treatment significantly improved bone microarchitectural parameters, including BMD and BV/TV, increased biomechanical strength at the tendon–bone junction, and promoted fibrocartilage formation with improved tissue organization. These findings are consistent with accumulating evidence that mesenchymal stem cell–derived exosomes exert potent regenerative effects in musculoskeletal tissues.

IGF1 has been shown to play a key role in tendon biology by promoting matrix synthesis, cell proliferation, and neovascularization [23,24]. In the present study, exosome treatment significantly enhanced neovascularization at the repair site, as evidenced by increased VEGF immunoreactivity and upregulated expression of angiogenic markers such as VEGF, CD31, and α-SMA. These pro-angiogenic effects were substantially attenuated when IGF1 was knocked down in the donor ADSCs, indicating that IGF1 is an essential mediator of exosome-induced angiogenesis. Improved vascularization is particularly critical at the rotator cuff tendon–bone interface, which is inherently hypovascular and prone to compromised healing.

Beyond structural and vascular regeneration, we found that ADSC-exosomes attenuates pyroptosis, a form of inflammatory cell death implicated in chronic tissue damage. The expression of GSDMD-N, a marker of pyroptosis [25], was elevated in injured tendons but significantly decreased with exosome treatment. Additionally, markers of NLRP3 inflammasome activation—including NLRP3, ASC, and cleaved caspase-1-were suppressed by exosome therapy, indicating that ADSC-derived exosomes modulate early inflammatory signaling pathways. IGF1 knockdown largely diminished these effects, further highlighting its central role in the anti-pyroptotic and anti-inflammatory action of exosomes.

Collectively, our findings suggest that IGF1 within ADSC-derived exosomes is not merely a positive biomarker, but rather a functionally active cargo that contributes substantially to therapeutic efficacy. Rather than acting through a single pathway, exosomal IGF1 appears to participate in a coordinated, multifaceted regenerative process that includes enhancement of angiogenesis, suppression of inflammasome-driven inflammation and pyroptosis, and support of extracellular matrix remodeling. Such integrative regulation is particularly advantageous in complex tendon–bone interfaces, where successful healing requires tightly coordinated cellular and molecular responses.

Several limitations of this study should be acknowledged. First, the experiments were conducted in a rat model, and although this model is well established, healing dynamics differ between rodents and humans. Validation in large animal models will be necessary before clinical translation. Second, the present study focused on short- to mid-term outcomes (1–8 weeks), and long-term evaluation of tendon integrity, mechanical durability, and re-tear rates remains to be performed. Third, while we identified IGF1 as a key functional component of ADSC-derived exosomes, the downstream signaling pathways in recipient cells—such as PI3K–Akt or MAPK signaling—were not directly investigated. Future studies should explore the cell-type–specific mechanisms by which IGF1-containing exosomes influence tenocytes, endothelial cells, macrophages, and resident stem cells. Finally, although systemic (tail vein) administration was selected for its clinical feasibility and was shown to allow exosomes to reach the tendon tissue, alternative local or biomaterial-assisted delivery strategies may further enhance therapeutic efficiency and warrant future investigation.

5. Conclusions

In conclusion, this study identifies IGF1 as a key bioactive component of ADSC-derived exosomes and demonstrates their therapeutic potential as a cell-free strategy for promoting tendon–bone healing after rotator cuff injury. By enhancing angiogenesis, suppressing inflammation and pyroptosis, and improving structural and mechanical integration at the tendon–bone interface, IGF1-containing exosomes significantly improve repair outcomes in a preclinical model. These findings provide a strong rationale for the further translational development of engineered exosome-based therapies for musculoskeletal regeneration.

Availability of Data and Materials

The datasets generated and analyzed during the current study are available from the corresponding author on reasonable request.

Author Contributions

FW designed the research study and wrote the initial draft. WQ, YJ, HS, YL and FW conducted experiments. WQ and YJ analyzed the data. All authors contributed to editorial changes in the manuscript. All authors read and approved the final manuscript. All authors have participated sufficiently in the work and agreed to be accountable for all aspects of the work.

Ethics Approval and Consent to Participate

The study was approved by Shanghai Jiao Tong University Affiliated Sixth People's Hospital (KFJ200887), this study was performed in strict accordance with the NIH guidelines for the care and use of laboratory animals (NIH Publication No. 85-23 Rev. 1985).

Acknowledgment

Not applicable.

Funding

This research received no external funding.

Conflict of Interest

The authors declare no conflict of interest.

Supplementary Material

Supplementary material associated with this article can be found, in the online version, at https://doi.org/10.31083/FBL47168.

References

[1] Oh JH, Park MS, Rhee SM. Treatment Strategy for Irreparable Rotator Cuff Tears. Clinics in Orthopedic Surgery. 2018; 10: 119–134. https://doi.org/10.4055/cios.2018.10.2.119.

[2] Samim M, Beltran L. The Postoperative Rotator Cuff. Magnetic Resonance Imaging Clinics of North America. 2020; 28: 181–194. https://doi.org/10.1016/j.mric.2019.12.003.

[3] Graham P. Rotator Cuff Arthropathy. Orthopedic Nursing. 2024; 43: 238–241. https://doi.org/10.1097/NOR.0000000000001047.

[4] Dickinson RN, Kuhn JE. Nonoperative Treatment of Rotator Cuff Tears. Physical Medicine and Rehabilitation Clinics of North America. 2023; 34: 335–355. https://doi.org/10.1016/j.pmr.2022.12.002.

[5] Di Benedetto P, Mancuso F, Tosolini L, Buttironi MM, Beltrame A, Causero A. Treatment options for massive rotator cuff tears: a narrative review. Acta Bio-medica: Atenei Parmensis. 2021; 92: e2021026. https://doi.org/10.23750/abm.v92iS3.11766.

[6] Mazini L, Rochette L, Admou B, Amal S, Malka G. Hopes and Limits of Adipose-Derived Stem Cells (ADSCs) and Mesenchymal Stem Cells (MSCs) in Wound Healing. International Journal of Molecular Sciences. 2020; 21: 1306. https://doi.org/10.3390/ijms21041306.

[7] Qin Y, Ge G, Yang P, Wang L, Qiao Y, Pan G, *et al*. An Update on Adipose-Derived Stem Cells for Regenerative Medicine: Where Challenge Meets Opportunity. Advanced Science (Weinheim, Baden-Wurttemberg, Germany). 2023; 10: e2207334. https://doi.org/10.1002/advs.202207334.

[8] Bacakova L, Zarubova J, Travnickova M, Musilkova J, Pajorova J, Slepicka P, *et al*. Stem cells: their source, potency and use in regenerative therapies with focus on adipose-derived stem cells - a review. Biotechnology Advances. 2018; 36: 1111–1126. https://doi.org/10.1016/j.biotechadv.2018.03.011.

[9] An Y, Lin S, Tan X, Zhu S, Nie F, Zhen Y, *et al*. Exosomes from adipose-derived stem cells and application to skin wound healing. Cell Proliferation. 2021; 54: e12993. https://doi.org/10.1111/cpr.12993.

[10] Song Y, You Y, Xu X, Lu J, Huang X, Zhang J, *et al*. Adipose-Derived Mesenchymal Stem Cell-Derived Exosomes Biopotentiated Extracellular Matrix Hydrogels Accelerate Diabetic Wound Healing and Skin Regeneration. Advanced Science (Weinheim, Baden-Wurttemberg, Germany). 2023; 10: e2304023. https://doi.org/10.1002/advs.202304023.

[11] Zhang Y, Liu T. Adipose-derived stem cells exosome and its potential applications in autologous fat grafting. Journal of Plastic, Reconstructive & Aesthetic Surgery: JPRAS. 2023; 76: 219–229. https://doi.org/10.1016/j.bjps.2022.10.050.

[12] Wang T, Li T, Niu X, Hu L, Cheng J, Guo D, *et al*. ADSC-derived exosomes attenuate myocardial infarction injury by promoting miR-205-mediated cardiac angiogenesis. Biology Direct. 2023; 18: 6. https://doi.org/10.1186/s13062-023-00361-1.

[13] Hu N, Cai Z, Jiang X, Wang C, Tang T, Xu T, *et al*. Hypoxia-pretreated ADSC-derived exosome-embedded hydrogels promote angiogenesis and accelerate diabetic wound healing. Acta Biomaterialia. 2023; 157: 175–186. https://doi.org/10.1016/j.actbio.2022.11.057.

[14] Shi J, Yao H, Chong H, Hu X, Yang J, Dai X, *et al*. Tissue-engineered collagen matrix loaded with rat adipose-derived stem cells/human amniotic mesenchymal stem cells for rotator cuff tendon-bone repair. International Journal of Biological Macromolecules. 2024; 282: 137144. https://doi.org/10.1016/j.ijbiomac.2024.137144.

[15] Ren Y, Zhang S, Wang Y, Jacobson DS, Reisdorf RL, Kuroiwa T, *et al*. Effects of purified exosome product on rotator cuff tendon-bone healing in vitro and in vivo. Biomaterials. 2021; 276: 121019. https://doi.org/10.1016/j.biomaterials.2021.121019.

[16] Zou J, Yang W, Cui W, Li C, Ma C, Ji X, *et al*. Therapeutic potential and mechanisms of mesenchymal stem cell-derived exosomes as bioactive materials in tendon-bone healing. Journal of Nanobiotechnology. 2023; 21: 14. https://doi.org/10.1186/s12951-023-01778-6.

[17] Huang Y, He B, Wang L, Yuan B, Shu H, Zhang F, *et al*. Bone marrow mesenchymal stem cell-derived exosomes promote rotator cuff tendon-bone healing by promoting angiogenesis and regulating M1 macrophages in rats. Stem Cell Research & Therapy. 2020; 11: 496. https://doi.org/10.1186/s13287-020-02005-x.

[18] Isazadeh M, Amandadi M, Haghdoust F, Lotfollazadeh S, Orzáez M, Hosseinkhani S. Split-luciferase complementary assay of NLRP3 PYD-PYD interaction indicates inflammasome formation during inflammation. Analytical Biochemistry. 2022; 638: 114510. https://doi.org/10.1016/j.ab.2021.114510.

[19] de Almeida L, Devi S, Indramohan M, Huang QQ, Ratsimandresey RA, Pope RM, *et al*. POP1 inhibits MSU-induced inflammasome activation and ameliorates gout. Frontiers in Immunology. 2022; 13: 912069. https://doi.org/10.3389/fimmu.2022.912069.

[20] Narayanan KB, Park HH. Purification and analysis of the interactions of caspase-1 and ASC for assembly of the inflammasome. Applied Biochemistry and Biotechnology. 2015; 175: 2883–2894. https://doi.org/10.1007/s12010-014-1471-4.

[21] Adler RS. Postoperative rotator cuff. Seminars in Musculoskeletal Radiology. 2013; 17: 12–19. https://doi.org/10.1055/s-0033-1333909.

[22] Avendano JP, Pereira D. Treatment of Calcific Tendonitis of the Rotator Cuff: An Updated Review. Orthopedics. 2023; 46: e326–e332. https://doi.org/10.3928/01477447-20230901-01.

[23] Liu L, Li X. A Review of IGF1 Signaling and IGF1-related Long Noncoding RNAs in Chemoresistance of Cancer. Current Cancer Drug Targets. 2020; 20: 325–334. https://doi.org/10.2174/1568009620666200228123754.

[24] Bi R, Luo X, Li Q, Li P, Li H, Fan Y, *et al*. Igf1 Regulates Fibrocartilage Stem Cells, Cartilage Growth, and Homeostasis in the Temporomandibular Joint of Mice. Journal of Bone and Mineral Research: the Official Journal of the American Society for Bone and Mineral Research. 2023; 38: 556–567. https://doi.org/10.1002/jbmr.4782.

[25] Kuang L, Wu Y, Shu J, Yang J, Zhou H, Huang X. Pyroptotic Macrophage-Derived Microvesicles Accelerate Formation of Neutrophil Extracellular Traps *via* GSDMD-N-expressing Mitochondrial Transfer during Sepsis. International Journal of Biological Sciences. 2024; 20: 733–750. https://doi.org/10.7150/ijbs.87646.